# JOINT SPACE PD CONTROL IN TERMS OF QUASI-VELOCITIES

**Krzysztof Kozłowski and Przemysław Herman***

* *Poznań University of Technology, Chair of Control, Robotics, and Computer Science, 60-965 Poznań, ul.Piotrowo 3A, POLAND*

Abstract: This paper presents new control algorithms for manipulators whose dynamics is expressed in terms of quasi-velocities (Jain and Rodriguez, 1995). Robot dynamic algorithms in terms of quasi-velocities are recursive in nature and consists of two recursions: one starts from a base of the manipulator towards its tip and the second in opposite direction. Both recursions are described by using vector-matrix notation. The considered algorithms allow to achieve end point of trajectory described in joint space of manipulator and in terms of quasi-velocities. The algorithms were tested experimentally on a two degrees of freedom manipulator.

Keywords: Robotics; Robot control; PD controllers; Joint trajectories; Matrix equations.

## 1. NOMENCLATURE

$\mathcal{N}$ number of joins and number of degrees of freedom,
$\theta \in R^{\mathcal{N}}$ vector of generalized positions,
$\dot{\theta}(k) \in R^{\mathcal{N}}$ vector of generalized velocities,
$(.)^T$ transpose operation,
$H^T(k) \in R^6$ joint map matrix for the $k$-th joint,
$\tau(k)$ vector of generalized force at $k$-th joint,
$M(\theta) \in R^{\mathcal{N}\times\mathcal{N}}$ mass matrix of the manipulator,
$C(\theta,\dot{\theta}) \in R^{\mathcal{N}}$ vector of Coriolis and centrifugal forces in standard equations of motion,
$\nu \in R^{\mathcal{N}}$ vector of normalized quasi-velocities,
$\xi \in R^{\mathcal{N}}$ vector of unnormalized quasi-velocities,
$C(\theta,\nu) \in R^{\mathcal{N}}$ vector of Coriolis and centrifugal forces in diagonalized normalized equations of motion,
$C(\theta,\xi) \in R^{\mathcal{N}}$ vector of Coriolis and centrifugal forces in diagonalized unnormalized equations of motion,
$m(\theta) \in R^{\mathcal{N}\times\mathcal{N}}$ spatial operator,
$T \in R^{\mathcal{N}}$ vector of generalized forces with elements $\tau(k)$,
$\epsilon \in R^{\mathcal{N}}$ vector of normalized quasi-moments,
$\kappa \in R^{\mathcal{N}}$ vector of unnormalized quasi-moments,
$H \in R^{\mathcal{N}\times 6\mathcal{N}}$ projection operator for all joint axes,
$\phi \in R^{6\mathcal{N}\times 6\mathcal{N}}$ rigid manipulator force transformation matrix,
$\psi \in R^{6\mathcal{N}\times 6\mathcal{N}}$ articulated manipulator force transformation matrix,
$K \in R^{6\mathcal{N}\times\mathcal{N}}$ shifted Kalman gain matrix,
$P \in R^{6\mathcal{N}\times 6\mathcal{N}}$ articulated inertia matrix,
$D = HPH^T \in R^{\mathcal{N}\times\mathcal{N}}$ articulated inertia about joint axes matrix.

## 2. INTRODUCTION

Globally diagonalized dynamics rarely exist in practice for multibody systems like manipulators (Jain and Rodriguez, 1995). Jain and Rodriguez have proposed, instead of transformation in configuration space, a diagonalizing transformation in velocity space. They have presented a diagonalized equation of motion. In this paper we consider two new control algorithms (in terms of normalized and unnormalized quasi-velocities). Results of simulation research for different algorithms in terms of quasi-velocities with gravitational forces

can be found in (Kozlowski and Herman, 1999a; Kozlowski and Herman 1999b). This paper is organized as follows. In next section diagonalized equation of motion and new control algorithms in quasi-velocity space are described. Simulation results are presented in the fourth section and results of experiments in the fifth section. The last section contains concluding remarks.

## 3. DIAGONALIZED EQUATIONS OF MOTION AND NEW CONTROLS

Consider a serial manipulator with $\mathcal{N}$ rigid links. The links of manipulator are numbered in increasing order from its tip to the base. The most outer link is link 1 and the most inner link is link $\mathcal{N}$. The basic properties of spatial operators were given in (Jain and Rodriguez, 1995). According to (Jain and Rodriguez, 1995) we can factorize mass matrix as: $M(\theta) = m(\theta)m^T(\theta)$.

As a consequence a kinetic energy of the system is written as:

$$\mathcal{K}(\theta,\dot{\theta}) = \frac{1}{2}\dot{\theta}^T m(\theta)m^T(\theta)\dot{\theta} = \frac{1}{2}\nu^T\nu \qquad (1)$$

where $\nu$ is a new vector of normalized quasi-velocities:

$$\nu = m^T(\theta)\dot{\theta} = D^{\frac{1}{2}}[I + H\phi K]^T\dot{\theta}. \qquad (2)$$

From (2) we can write the vector of generalized velocities as (Jain and Rodriguez, 1995):

$$\dot{\theta} = \ell^T(\theta)\nu = [I - H\psi K]^T D^{-\frac{1}{2}}\nu. \qquad (3)$$

New equations of motion in $(\theta,\nu)$ coordinates according to (Jain and Rodriguez, 1995) are:

$$\dot{\nu} + C(\theta,\nu) = \epsilon, \qquad (4)$$

$$\epsilon = \ell(\theta)T = D^{-\frac{1}{2}}[I - H\psi K]T, \qquad (5)$$

$$T = [I + H\phi K]D^{\frac{1}{2}}\epsilon. \qquad (6)$$

According to (Jain and Rodriguez, 1995) the Coriolis term $C(\theta,\nu)$ is orthogonal to the generalized velocities $\nu$ and therefore does no mechanical work $\nu^T C(\theta,\nu) = 0$.

In this work we consider system with gravity and the equations of motion are written as (in terms of normalized quasi-velocities):

$$\dot{\nu} + C(\theta,\nu) + G_\nu(\theta) = \epsilon \qquad (7)$$

where $G_\nu(\theta) = m^{-1}(\theta)G(\theta)$ and $G(\theta)$ - gravitational forces in standard equations of motion.

A kinetic energy of the system using vector of unnormalized quasi-velocities $\xi$ is defined as:

$$\mathcal{K} = \frac{1}{2}\xi^T D(\theta)\xi. \qquad (8)$$

New equations of motion in terms of $(\theta,\xi)$ coordinates according to (Jain and Rodriguez, 1995) are:

$$D\dot{\xi} + C(\theta,\xi) = \kappa. \qquad (9)$$

Here we consider (as earlier) system with gravity and the equations of motion in terms of unnormalized quasi-velocities are written as:

$$D\dot{\xi} + C(\theta,\xi) + G_\xi(\theta) = \kappa \qquad (10)$$

where $G_\xi(\theta) = D^{\frac{1}{2}}m^{-1}(\theta)G(\theta)$ and $G(\theta)$ - gravitational forces in standard equations of motion.

In case of normalized and unnormalized quasi-velocities we propose the following control algorithms:

PROPOSITION 1 and 2.

$$\epsilon = -c_1\nu + m^{-1}(\theta)c_2\tilde{\theta} + G_\nu(\theta) \qquad (11)$$

$$\kappa = -c_1\xi + D^{\frac{1}{2}}m^{-1}(\theta)c_2\tilde{\theta} + G_\xi(\theta) \qquad (12)$$

where $c_1$ and $c_2$ are positive definite diagonal gain matrices and $\tilde{\theta} = \theta_d - \theta$. Equations (11) and (12) have PD structure in internal space of manipulator in terms of normalized and unnormalized quasi-velocities, respectively.

Recall that (Sciavicco and Siciliano, 1996) classical equations of motion are:

$$M(\theta)\ddot{\theta} + C(\theta,\dot{\theta}) + G(\theta) = u. \qquad (13)$$

PD control algorithm for this structure is:

$$u = -c_1\dot{\theta} + c_1\dot{\theta} + G(\theta) \qquad (14)$$

where $\tilde{\theta} = \theta_d - \theta$ is the joint error between the desired and actual posture.

Comparing PD structure in quasi-variables with classical one can notice that the first term is different due to the fact that we use quasi-velocities instead of joint velocities. In the second term of operator $m(\theta)$ appear kinematical and dynamical variables.

The main difference between PD control algorithms in normalized and unnormalized variables relies on a different quasi-velocity $\xi = D^{-\frac{1}{2}}\nu$ (Jain and Rodriguez, 1995). Because of that the dynamics of both systems is not the same.

## 4. SIMULATION RESULTS

In this section we present simulation results for manipulator KARI-2 consisting of two degrees of freedom (double pendulum) in horizontal plane. The KARI-2 robot is characterized by the following set of manipulator parameters:

- links masses: $m_1 = 0.75kg, m_2 = 7.92kg$;
- link inertias: $J_1 = 0.359kgm^2, J_2 = 2.597kgm^2$;
- distance axis of rotation - mass center: $p_1 = 0.28m, p_2 = 0.5235m$;
- length of links: $l_1 = 0.525m, l_2 = 0.595m$;
- static moments: $m_1p_1 = 0.21kgm, m_2p_2 = 4.146kgm$.

During simulations we have chosen a desired sinusoidal trajectories (in joint space of manipulator) as follows:

$$\theta_{1d} = \frac{\pi}{4}\sin(\frac{\pi}{3}t),\ \theta_{2d} = \frac{\pi}{10}\sin(\frac{\pi}{3}t). \quad (15)$$

The following configuration values were chosen as starting joint variables: $\theta_1 = \theta_2 = 0[rad]$. ($\theta_2 = 0[rad]$ is not kinematic singular point). As a 2-nd trajectory used for simulation we have chosen spline parabolic-linear trajectory (SPLT) with $\theta_1 = \theta_2 = 0 \div \frac{1}{4}\pi[rad]$ with time duration $t_f = 7[s]$ and acceleration $\ddot{\theta}_1 = \ddot{\theta}_2 = \frac{\pi}{40}[rad/s^2]$ Simulations were performed using SIMULINK (with integration fixed step size $0.005[s]$ and Dormand-Prince method), and control coefficients (for normalized and unnormalized case):

$$c_D(1) = c_D(2) = 50, c_P(1) = c_P(2) = 1500. (16)$$

We also used two input coefficients equal 0.001 and two output coefficients equal 1000, respectively.

The choice of these coefficients is very important because if $c_D$ is small, then variables tend to the steady values slowly. If they have large values, then variables quickly tend to steady state values. Sometimes the system may be not physically realized.

Simulation results for sinusoidal trajectories (ST) are presented in Figures 1 to 5, and for SLPT in Figures 6 to 10. In Figures 1 and 6 the desired trajectories $th1d, th2d$ in joint space are shown. Figures 2 and 7 show orientation errors for the first joint. For ST it is about $0.03[rad]$ for classical case and about $0.015 - 0.04[rad]$ for quasi-velocity case. For SLPT errors are smaller i.e. $5.5 \cdot 10^{-3}$ for classical case, $4.5 \cdot 10^{-3}$ and $12 \cdot 10^{-3}$ for normalized and unnormalized cases, respectively, and tend to zero. Figures 3 and 8 show orientation errors at the second joint. For ST they are about $0.01[rad]$ for classical case and $0.05 - 0.07[rad]$ for quasi-velocity case, respectively. For SLPT errors are smaller i.e. $0.005[rad]$ for classical case and about $0.02[rad]$ for quasi-velocity case but they tend to zero. We can get smaller values of errors if we increase control coefficients but it is more difficult in this case to compare simulation and experimental results. Notice that the errors for quasi-velocity cases accumulate. In Figures 4 and 9 we can see moments $tau1$ in the first joint. After a short time this moment is equal about $5[Nm]$ (for ST).

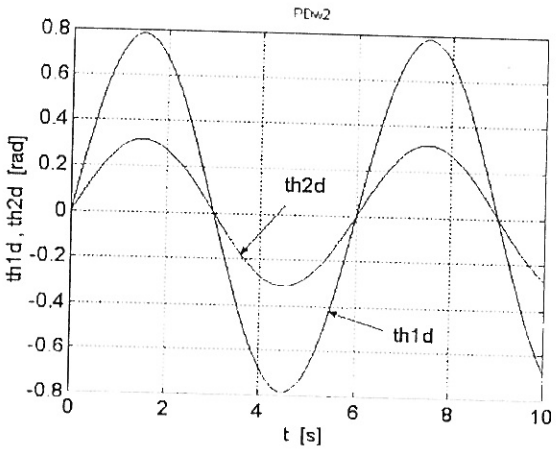


Fig. 1. Results of simulation: desired trajectories in joint space.

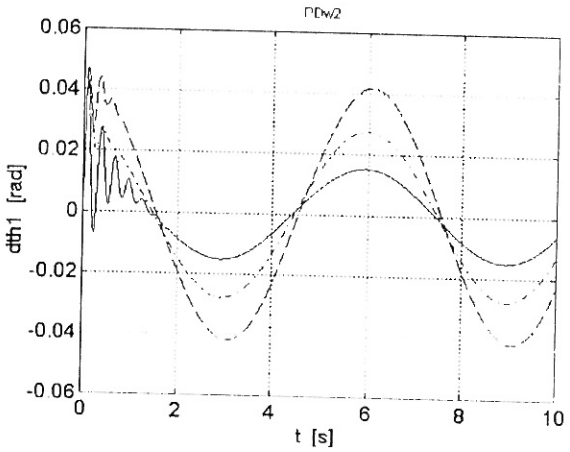


Fig. 2. Results of simulation: orientation errors $dth1$. Lines: dashdot line - classical case, solid line - normalized case, dashed line - unnormalized case.

Maximal value for SLPT is about $0.3 - 0.4[Nm]$. In Figures 5 and 10 a comparison between real moment and quasi-moments (normalized and unnormalized) is shown. Simulation indicates that use of PD controllers give better results for SLPT.

## 5. EXPERIMENTAL RESULTS

The same kind of robot i.e. KARI-2 was investigated experimentally using dSPACE-tools. Instead of dynamical model of manipulator a DSP card was inserted.

Experimental results were obtained using SIMULINK-programme with control coefficients (fixed step size $0.001[s]$ and Dormand-Prince method):

$$c_D(1) = c_D(2) = 1, c_P(1) = c_P(2) = 1500. (17)$$

We also used two input coefficients equal 0.001 and two output coefficients equal 1000, respectively.

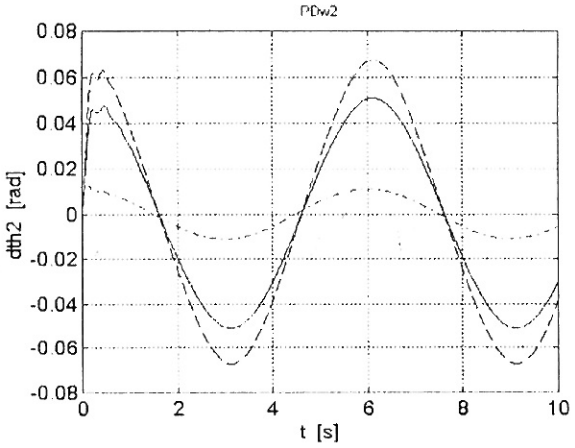


Fig. 3. Results of simulation: orientation errors $dth2$. Lines: dashdot line - classical case, solid line - normalized case, dashed line - unnormalized case.

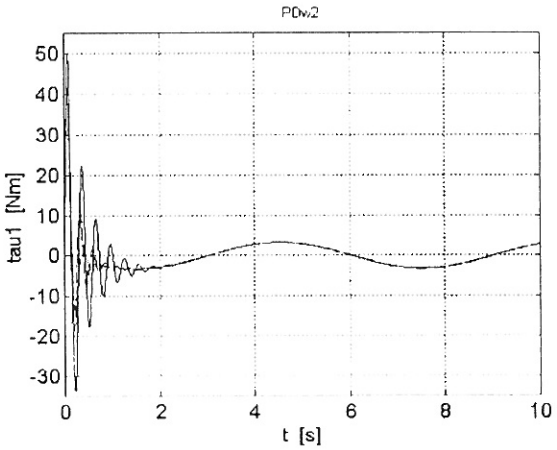


Fig. 4. Results of simulation: moments in the first joint $\tau_1$. Lines: dashdot line - classical case, solid line - normalized case, dashed line - unnormalized case.

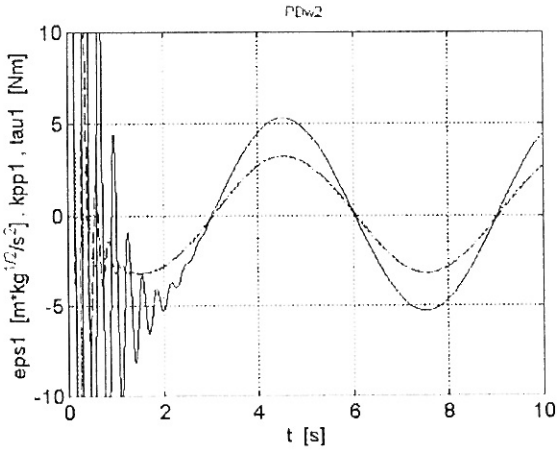


Fig. 5. Results of simulation: comparison between moment $\tau_1$, quasi-moments $\epsilon_1$, and $\kappa_1$. Lines: dashdot line - classical case, solid line - normalized case, dashed line - unnormalized case.

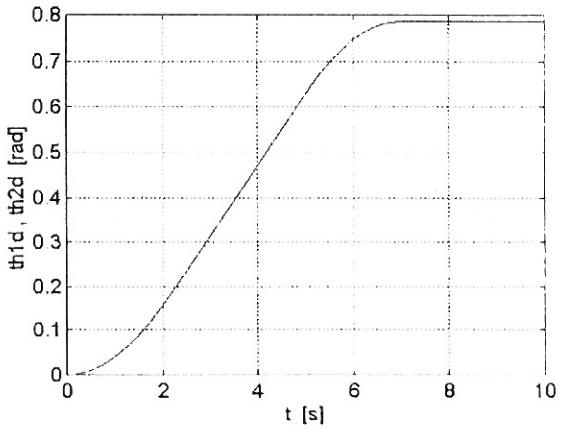


Fig. 6. Results of 2-nd simulation: desired trajectories in joint space.

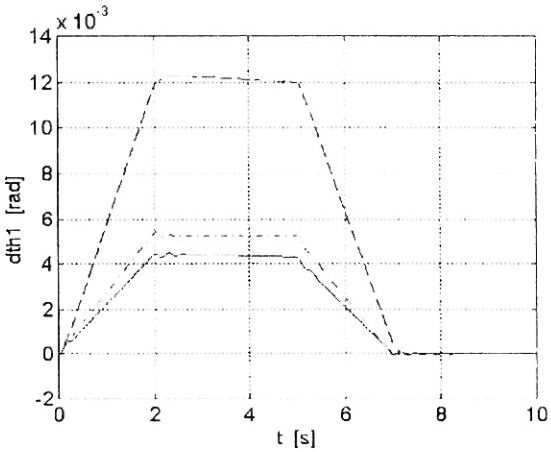


Fig. 7. Results of 2-nd simulation: orientation errors $dth1$. Lines: dashdot line - classical case, solid line - normalized case, dashed line - unnormalized case.

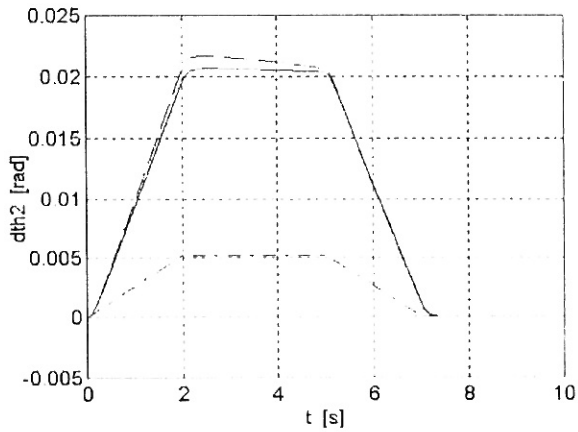


Fig. 8. Results of 2-nd simulation: orientation errors $dth2$. Lines: dashdot line - classical case, solid line - normalized case, dashed line - unnormalized case.

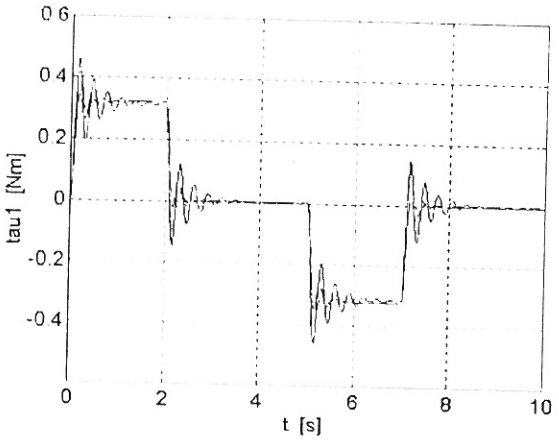


Fig. 9. Results of 2-nd simulation: moments in the first joint $\tau_1$. Lines: dashdot line - classical case, solid line - normalized case, dashed line - unnormalized case.

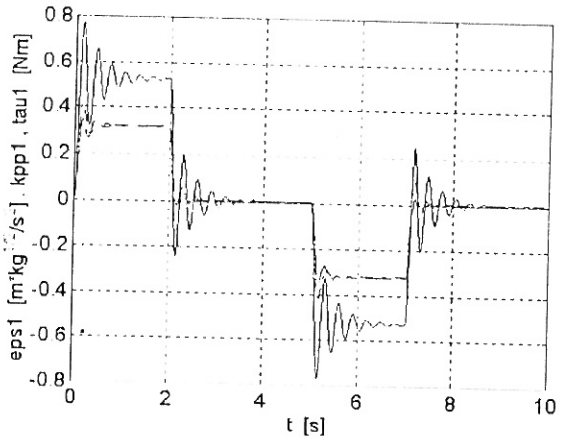


Fig. 10. Results of 2-nd simulation: comparison between moment $\tau_1$, quasi-moments $\epsilon_1$, and $\kappa_1$. Lines: dashdot line - classical case, solid line - normalized case, dashed line - unnormalized case.

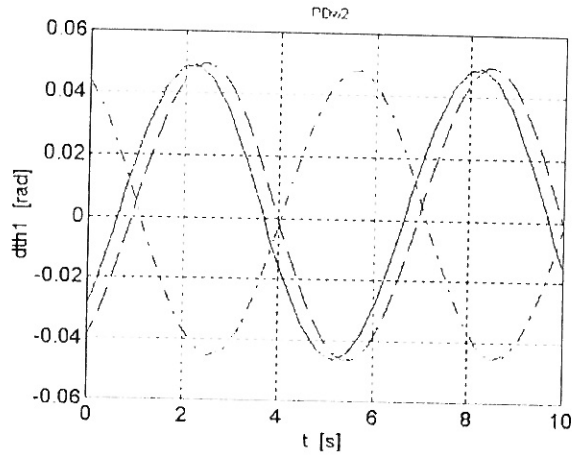


Fig. 11. Results of experiment: orientation errors $dth1$. Lines: dashdot line - classical case, solid line - normalized case, dashed line - unnormalized case.

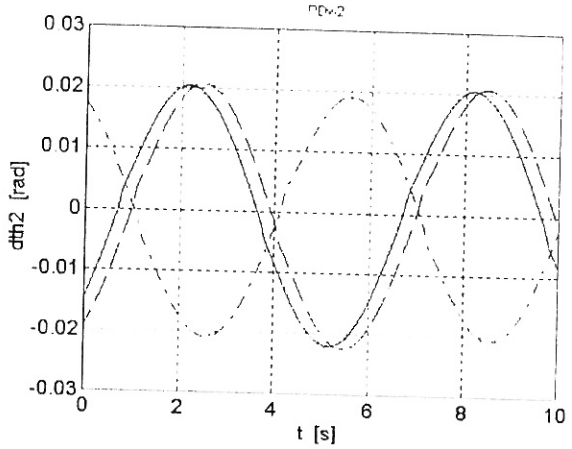


Fig. 12. Results of experiment: orientation errors $dth2$. Lines: dashdot line - classical case, solid line - normalized case, dashed line - unnormalized case.

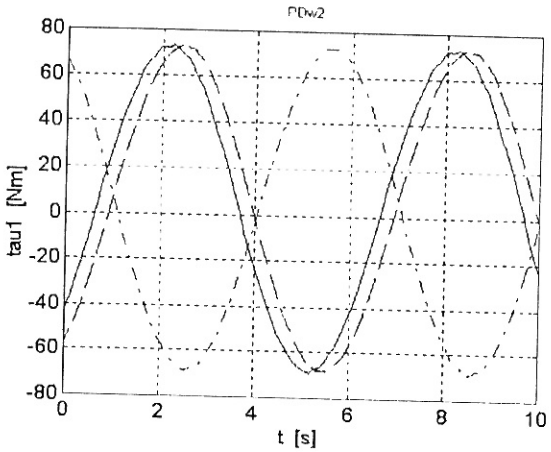


Fig. 13. Results of experiment: moments in the first joint $\tau_1$. Lines: dashdot line - classical case, solid line - normalized case, dashed line - unnormalized case.

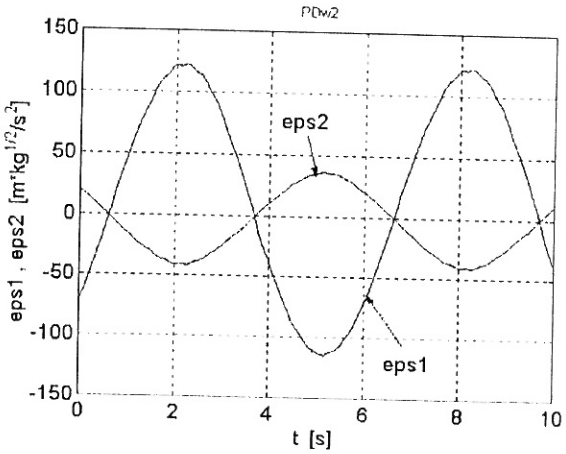


Fig. 14. Results of experiment: normalized quasi-moment $\epsilon_1, \epsilon_2$.

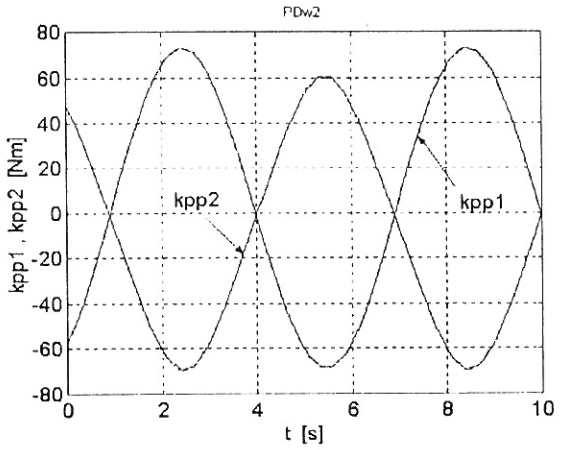


Fig. 15. Results of experiment: unnormalized quasi-moment $\kappa_1, \kappa_2$.

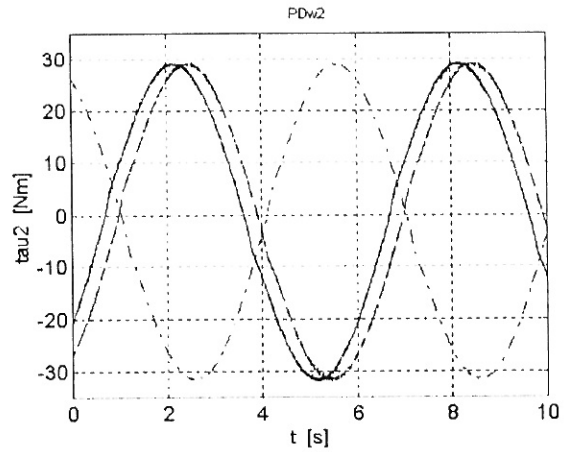


Fig. 16. Results of experiment: moments in the second joint $\tau_2$. Lines: dashdot line - classical case, solid line - normalized case, dashed line - unnormalized case.

The experimental results obtained with dSPACE-tools are presented in Figures 11 to 16 (desired trajectories $th1d, th2d$ in joint space are similar as in simulation). Figure 11 shows orientation errors for the first joint. They are about $0.05[rad]$. For all cases errors are comparable. Figure 12 shows orientation errors for the second joint. They are about $0.02[rad]$ and also comparable amplitude. In Figure 13 we can see moments $tau1$ in first joint. The moments are comparable in all cases but their values are higher than in simulation. In Figures 14 and 15 a comparison between real moment and quasi-moments (normalized and unnormalized) are shown. In normalized case $eps1$ has higher value than real moment and in unnormalized case $kpp1$ has similar value as $tau1$. In Figure 16 we can see moments in the second joint. They are similar in all cases and have smaller values than for the first joint because input signals have not high amplitude.

## 6. CONCLUDING REMARKS

Results of research obtained in simulation and experimental way (using SIMULINK and dSpace) indicate that we can realize effective control in quasi-velocity space. We examined that in experiment PD controller in terms of quasi-velocities in joint space give comparable results in experiment. These results are similar as for classical PD controller in literature (Niemeyer and Slotine, 1991; Slotine and Li, 1987). In (Niemeyer and Slotine, 1991) PD controller for fast sinusoidal trajectory (faster as here and for other type of manipulator) had in experiment orientation errors about $0.10 - 0.17[rad]$. In simulation moments have smaller values than in experiment due to higher values of coefficients in simulation. Note, that the manipulator is real but control algorithms take place in an abstract space. Because of that we transform physical variables into quasi-velocity space and at the end we transform quasi-moments into physical moments which are input values of the manipulator. Other control structures are also possible. Results of further investigations will be presented in next papers.

## REFERENCES

Jain A., G. Rodriguez (1995). Diagonalized Lagrangian Robot Dynamics, *IEEE Transactions on Robotics and Automation*, Vol.11, No 4, pp.571-584.

Kozłowski K., P. Herman (1999a). A New Control Algorithm in Terms of Normalized Quasi-Velocities with Gravitational Forces, *Proc. of the First Workshop on Robot Motion and Control RoMoCo'99*, June 28-29, Kiekrz, Poland, pp.95-100.

Kozłowski K., P. Herman (1999b). A Control in Terms of Unnormalized Quasi-Velocities with Gravititional Forces, *Proc. of 1999 IEEE International Conference on Intelligent Engineering Systems*, November 1-3, Poprad, High Tatras, Stara Lesna, Slovakia, pp.51-55.

Niemeyer G., J.J. Slotine (1991). Performance in Adaptive manipulator Control, *The Int. Journal of Robotics Research*, Vol.10, No.2, pp.149-161.

Sciavicco L., B. Siciliano (1996). *Modeling and Control of Robot Manipulators*. The McGraw-Hill Companies, Inc., New York.

Slotine J.J., W. Li (1987). On the Adaptive Control of Robot Manipulators, *The Int. Journal of Robotics Research*, Vol.6, No.3, pp.49-59.